Jorge Álvarez; Jorge Ruiz; Miguel Bernal

A family of Lyapunov-based control schemes for maximum power point tracking in buck converters

Kybernetika, Vol. 59 (2023), No. 2, 294–313

Persistent URL: http://dml.cz/dmlcz/151697

KYBERNETIKA — VOLUME *59* (2023), NUMBER 2, PAGES 294–313

A FAMILY OF LYAPUNOV-BASED CONTROL SCHEMES FOR MAXIMUM POWER POINT TRACKING IN BUCK CONVERTERS

Jorge Álvarez, Jorge Ruiz, and Miguel Bernal

This paper presents a novel family of Lyapunov-based controllers for the maximum power point tracking problem in the buck converter case. The solar power generation system here considered is composed by a stand-alone photovoltaic panel connected to a DC/DC buck converter. Lyapunov function candidates depending on the output are considered to develop conditions which, in some cases, can be expressed as linear matrix inequalities; these conditions guarantee that the output goes asymptotically to zero, thus implying that the MPPT is achieved. Simulation and real-time results are presented, which validate the effectiveness of the proposals.

Keywords: solar energy, photovoltaic panel, maximum power point tracking, Lyapunov method, convex model, linear matrix inequalities

Classification: 93D30, 47N70, 93C10

1. INTRODUCTION

Fossil fuel-based energy sources emit large amounts of greenhouse gases, making them the main cause of global warming; therefore, the interest in renewable energy has increased in recent years [12, 22]. The main sources of renewable energy are wind [21], biomass, and solar, their main advantages being low maintenance cost, non-pollution characteristics, and their non-decreasing availability [5, 25].

Solar energy sources consist in using the photovoltaic (PV) effect to transform solar energy into electrical one. Hence, being a constant source of energy, solar light can be used to meet ever-increasing energy needs. The energy generation of PV systems depends on weather conditions such as solar irradiation and temperature; for this reason, the problem of tracking the point of maximum power output (MPPT problem), which changes continuously during the day, is at the core of the efficient use of solar energy [14, 16]. The MPPT problem can be seen as a control tracking one, i. e., by means of a control input –duty cycle– a nonlinear output expression –the time derivative of the system power with respect to the PV voltage– is driven to 0 [1].

There exists a lot of MPPT techniques in the literature; they can be classified in two groups: those based on heuristics and algorithms (model-free) and those based on formal control techniques (model-based). The advantages of the former lie on their easier

DOI: 10.14736/kyb-2023-2-0294

design process, their intuitive physical appeal, and their readiness for practical implementability; in contrast, heuristics usually lack mathematical guarantees for stability and convergence of algorithms. Popular model-free techniques are perturb and observe (P&O) [28], incremental conductance (IC) [13], fractional open-circuit voltage (FV_{oc}) [8], fractional short circuit current (FSC) [27], neural networks [4] and fuzzy logic control [2]. The widely-used P&O algorithm is based on performing periodic disturbances (increases or decreases) in the panel voltage and measuring the difference between the voltage on the panel PV and the preceding perturbation cycle; a modification of this algorithm under partial shading conditions by integrating artificial bee colony algorithms is presented in [24].

On the other hand, model-based control schemes for solving the MPPT problem are scarce, due to the complexity of expressions and nonlinearities involved in the model of the DC-DC converter, especially when time-varying parameters and functions such as temperature and irradiation are fully taken into account. Usual options include linearization [18], Takagi–Sugeno blendings [10, 11], and Lyapunov-based design [26]; nevertheless, all sort of simplifications are made in them as standard feedback techniques cannot be directly applied. Some works mix algorithms and model-based approaches; they usually consider themselves model-based, though the assumptions and procedures in them rely on practical data and on-line decisions, e. g., [19].

Contribution: This work belongs to the model-based class of control schemes to solve the MPPT problem, considering a photovoltaic panel connected to DC/DC buck converter; it is Lyapunov-based, taking full nonlinear expressions and time-varying functions into account, and guaranteeing numerical obtention of gains via linear matrix inequalities (LMIs) [9], which can be solved in polynomial time via efficient algorithms already implemented in commercial software [15]. In contrast with other Lyapunov-based proposals such as the well-known Artstein's Theorem [3, 30], the proposal deals with systems with time-varying expressions and no equilibrium point at the origin. It is shown that, despite their complexity, several Lyapunov-based proposals can be successfully designed, simulated, and physically implemented, thanks to convex handling of nonlinear expressions, output-dependent Lyapunov functions, and availability of signals via proper measurements [6].

Organization: Section 2 introduces some preliminaries on Lyapunov theory, convex modelling, and linear matrix inequalities; Section 3 describes the MPPT setup this work is concerned with; it includes enough detail as to formulate the problem statement in the form of a nonlinear control challenge; Section 4 develops the Lyapunov-based control proposals for the MPPT problem in a theorem-like form; Section 5 presents the simulation results corresponding to the preceding theoretical proposals while real-time implementation results of some of them are shown in Section 6; finally, some conclusions and future work are discussed in Section 7.

2. PRELIMINARIES

In this section, basics on Lyapunov theory, convex rewriting of expressions, and linear matrix inequalities, are briefly described as they constitute the basis on which the results in this report are developed.

Lyapunov theory: Recall that an equilibrium point $x = 0$ of a system $\dot{x} = f(x)$ with $f(x)$ locally Lipschitz over a domain $D \subset \mathbb{R}^n$ such that $0 \in D$, is asymptotically stable if there exists a continuously differentiable function $V(x)$ defined over D such that $V(0) = 0$ with conditions $V(x) > 0$ and $\dot{V}(x) < 0$ holding $\forall x \neq 0$, $x \in D$. See [17, Theorem 3.3] for details. The same results apply for uniform asymptotic stability of equilibrium points of time-varying systems $\dot{x} = f(t, x)$ like the one under consideration, though the Lyapunov function is allowed to be time-varying, i. e., $V(t, x)$. See [7, Theorem B.3].

Convex embedding: Nonlinear scalar expressions $z(x)$ defined on a compact set $\mathcal{C}$ of the state space $\mathbb{R}^n$ can be written as convex sums of their bounds, i. e., defining $z^0 = \min_{x\in\mathcal{C}} z(x)$, $z^1 = \max_{x\in\mathcal{C}} z(x)$, $w_0(x) = (z^1 - z(x))/(z^1 - z^0)$, and $w_1(x) = 1 - w_0(x)$, it is obvious that $z(x) = w_0(x)z^0 + w_1(x)z^1$ with $w_0(x)$ and $w_1(x)$ being convex functions in $\mathcal{C}$.

Linear matrix inequalities: Problems that can be solved in polynomial time include linear programming and convex optimization; to the last sort of problems belong linear matrix inequalities, which can be efficiently solved via interior point algorithms already implemented in several toolboxes, e. g., the LMI Toolbox of MATLAB [15]. Their usual formulation is $F_0 + \sum_{i=1}^{m} x_i F_i > 0$, where x_i and F_0, F_i $i \in \{1, 2, \ldots, m\}$, are decision variables and constant matrices of adequate size [9]. A whole body of theory derived form combining convex embedding and the direct Lyapunov method is available for nonlinear control systems analysis and design [7].

In the sequel, the following acronyms will be employed:

MPPT	Maximum Power Point Tracking
PV	Photovoltaic
P&O	Perturb and Observe
DC/DC	Direct Current/Direct Current
LMI	Linear Matrix Inequalities
PDC	Parallel Distributed Compensation
IC	Incremental Conductance
FSC	Fractional Short Current

Tab. 1: Abbreviations.

3. PROBLEM STATEMENT

This section describes the photovoltaic array and the DC/DC buck converter under consideration, including their mathematical models. This set of PV array and buck converter is ideal for high irradiation regions and charging of low-voltage batteries. A problem statement is now made concerning the MPPT problem.

Consider a PV power control system with a buck converter as the one schematically shown in Figure 1; its dynamical model is given by the following 3rd-order nonlinear state-space representation [10]:

$$\begin{bmatrix}\dot{x}_1\\ \dot{x}_2\\ \dot{x}_3\end{bmatrix}=\begin{bmatrix}\left(R_b i_o-(R_b+R_L)x_1-x_3+(V_D+x_2)u-V_D\right)/L\\ (i_{pv}(x_2,T(t),\lambda(t))-x_1 u)/C_a\\ (x_1-i_o)/C_b\end{bmatrix} \tag{1}$$

where the states x_1, x_2, and x_3 are the current on the inductance L, the PV array output voltage (on the capacitance C_a), and the load voltage (on the capacitance C_b), respectively; u is the control signal corresponding to the duty cycle; constants R_b and R_L are the internal resistances on the capacitance C_b and the inductance L, respectively; constant V_D is the forward voltage of the power diode, i_o is the measurable load current, usually taken as $x_3/2$, and $i_{pv}(x_2,T(t),\lambda(t)) = n_p I_{ph}(t) - n_p I_{rs}(t)(e^{k_{pv}(t)x_2/n_s}-1)$ is the PV array output current for a panel composed of solar cells arranged in an n_p-parallel, n_s-series configuration, with $k_{pv}(t) = q/(pKT(t))$ where constant q is the electronic charge, constant p is the ideal p-n junction characteristic factor, K is the Boltzmann's constant, $\lambda(t)$ is the irradiation measured in mW/cm^2, $T(t)$ is the cell temperature measured in °C, $I_{ph}(t)$ is the light-generated current, and $I_{rs}(t)$ is the reverse saturation current; the latter two, I_{rs} and I_{ph}, depend on the irradiation $\lambda(t)$ and the temperature $T(t)$ via the following expressions:

$$\begin{aligned} I_{rs}(t) =& I_{rr}\left(\frac{T(t)}{T_r}\right)^3 e^{qE_{gp}(1/T_r-1/T(t))K/p},\\ I_{ph}(t) =& (I_{sc}+K_I(T(t)-T_r))\frac{\lambda(t)}{100}, \end{aligned}$$

where constant I_{rr} is the reverse saturation current at the reference temperature T_r, constant E_{gp} is the bandgap energy of the semiconductor making up the cell, constant I_{sc} is the short-circuit cell current at the reference temperature and irradiation, and constant K_I is the short-circuit current temperature coefficient. Importantly, only states x_1 and x_2, temperature $T(t)$ and irradiation $\lambda(t)$ are measurable. The parameters employed in this work are given in Table 2.

The array power is given by

$$P_{pv} = i_{pv}(x_2,T(t),\lambda(t))x_2 = n_p I_{ph}(t)x_2 - n_p I_{rs}(t)x_2(e^{k_{pv}(t)x_2/n_s}-1).$$

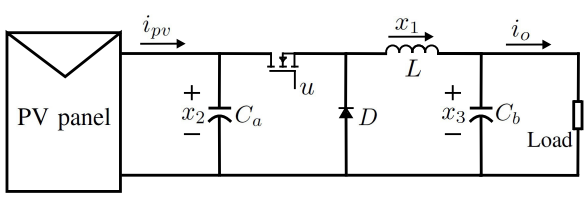

Fig. 1: PV power control system using a dc/dc buck converter.

Param.	Value	Param.	Value
q	1.6×10^{-19}C	T_r	25°C
p	1	E_{gp}	1.1
K	1.3805×10^{-23}J/K	I_{sc}	1.9A
I_{rr}	1.73×10^{-5}A	K_I	0.00114
n_p	1	n_s	72
C_a	1mF	R_L	4.1Ω
C_b	1mF	R_b	0.25Ω
L	200μH	V_D	0.57

Tab. 2: Parameters.

The maximum power point is attained at $dP_{pv}/dv_{pv} = 0$, where

$$\begin{aligned} y(t) \equiv & \frac{dP_{pv}}{dv_{pv}} = i_{pv}(x_2, T(t), \lambda(t)) + x_2 \frac{di_{pv}}{dx_2} \\ = & i_{pv}(x_2, T(t), \lambda(t)) - \frac{n_p k_{pv}(t)}{n_s} I_{rs} x_2 e^{k_{pv}(t) x_2 / n_s}. \end{aligned} \tag{2}$$

Numerical simulations and real-time implementations developed in this work consider the solar PV module DBF30 which characteristics of the power with respect to the voltage are shown in Fig 2, also it can be seen that the maximum power point depends on the different levels of irradiation and temperature.

Thus, the following problem statement can be made:

Control objective: The MPPT problem consists in finding $u(t)$ such that $\lim_{t\to\infty} y(t) = 0$ considering that states $x_1(t)$ and $x_2(t)$ as well as the temperature $T(t)$ and irradiance $\lambda(t)$ are measurable.

Note that $y(t)$ in (2) is a highly nonlinear expression and therefore implies a high degree of difficulty to employ it to find the maximum power point; this is the reason

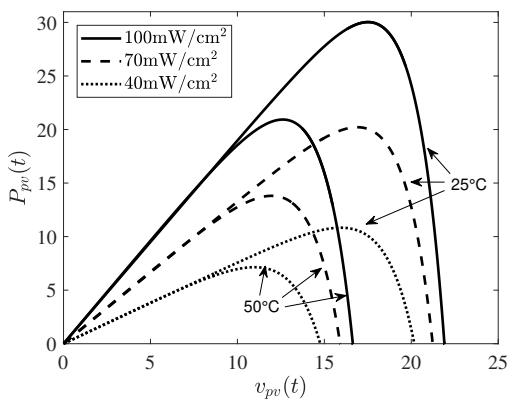

Fig. 2: Characteristics of the PV array: power with respect to the voltage.

behind the fact that most of researchers avoid directly dealing with it [10].

4. MAIN RESULTS

In this section, a family of Lyapunov-based control proposals for MPPT is developed. It is shown that, despite its complexity, output (2) can be driven to 0 by nonlinear control laws that employ measurable signals such as x_1 and x_2 as well as time-varying functions of temperature $T(t)$ and irradiance $\lambda(t)$; moreover, some of these schemes have fixed structures in the form of parallel distributed compensation (PDC) whose gains that can be obtained via LMIs [7].

System (1) is a 3rd-order time-varying affine-in-control nonlinear system which, along with its output (2), has a compact form

$$\dot{x}(t) = f(t,x) + g(x)u(t), \quad y(t) = h(t,x), \tag{3}$$

where

$$f(t,x) = \begin{bmatrix} \dfrac{R_b i_o - (R_b + R_L)x_1 - x_3 - V_D}{L} \\ i_{pv}(x_2, T(t), \lambda(t))/C_a \\ (x_1 - i_o)/C_b \end{bmatrix}, \; g(x) = \begin{bmatrix} \dfrac{V_D + x_2}{L} \\ \dfrac{-x_1}{C_a} \\ 0 \end{bmatrix},$$

$$h(t,x) = i_{pv}(x_2, T(t), \lambda(t)) - \frac{n_p k_{pv}(t)}{n_s} I_{rs} x_2 e^{k_{pv}(t)x_2/n_s}.$$

The main idea behind the next proposals is to find a Lyapunov function $V(y)$ guaranteeing $\lim_{t\to\infty} y(t) = 0$ by an appropriate choice of the duty cycle u: standard techniques propose $V(y)$ and deduce the corresponding u analytically; more systematic proposals adopt a structure for $V(y)$ and deduce u numerically by convex optimization techniques, e. g., LMIs. In the sequel, both standard and dynamical Lyapunov functions are found; all of them will be quadratic.

4.1. Lyapunov-based analytical proposals

Three analytical proposals are considered: a classical one employs a quadratic Lyapunov function candidate that depends exclusively on the output; the other two are based on time-varying Lyapunov functions which, despite its complexity, are more suitable for time-varying systems as the one under consideration.

4.1.1. A standard quadratic Lyapunov function

Consider the Lyapunov function candidate $V(y) = 0.5y^2$, which satisfies $V(0) = 0$ and $V(y) > 0 \; \forall y \neq 0$; its time derivative is given by

$$\begin{aligned} \dot{V} =& y\dot{y} = y \begin{bmatrix} \left(\dfrac{\partial h}{\partial x}\right)^T & \left(\dfrac{\partial h}{\partial t}\right)^T \end{bmatrix} \begin{bmatrix} f(t,x) + g(x)u \\ 1 \end{bmatrix}, \\ =& y \left(\frac{\partial h}{\partial x}\right)^T (f(t,x) + g(x)u) + \left(\frac{\partial h}{\partial t}\right)^T. \end{aligned}$$

Note that the output $h(t,x)$ in (3) can be seen as a function of time-varying temperature and irradiation as well as the state x_2; thus, $\left(\frac{\partial h}{\partial t}\right)T$ takes into account the referred dependencies. In order to guarantee $\lim_{t\to\infty} y(t) = 0$ it is enough to satisfy $\dot{V}(y) < 0$, $\forall y \neq 0$, $t \geq 0$, which can be accomplished by solving u from the following equation:

$$y\left(\frac{\partial h}{\partial x}\right)^T (f(t,x) + g(x)u) + \left(\frac{\partial h}{\partial t}\right)^T = -ky^2, \tag{4}$$

where $k > 0$ determines the rate of convergence for the Lyapunov function [23, 29]. Clearly, the solved u is a state-dependent time-varying control law, which tracks the maximum power point of the PV array; despite its complexity, such control law is fully implementable.

4.1.2. A dynamic quadratic Lyapunov function driven to a constant

As stated before, the time-varying nature of the system naturally asks for a time-varying Lyapunov function. To this end, a quadratic time-varying Lyapunov function candidate $V(t,y) = 0.5y^2p(t)$ is to be considered, such that $p(t) > 0$, $\forall t \geq 0$; the latter requisite will be guaranteed by imposing adequate dynamics from an initial condition $p(0) > 0$. Thus,

$$\dot{V}(t,y) = y\dot{y}p(t) + 0.5y^2\dot{p}(t),$$

which, again, can be made negative $\forall y \neq 0$, $\forall t \geq 0$ if $\dot{V}(t,y) = -kV(t,y)$, with $k > 0$, i. e.

$$y\dot{y}p(t) + 0.5y^2\dot{p}(t) = -0.5ky^2p(t),$$

from which the dynamics of $p(t)$ can be solved as

$$\dot{p}(t) = -\left(k + 2\frac{\dot{y}}{y}\right)p(t), \quad y \neq 0.$$

The time derivative of output y involves input u (via $\dot{x}_2$), which means it has a structure of the form $\dot{y} = \bar{y}_1(t,x)u + \bar{y}_2(t,x)$, where expression $\bar{y}_1(t,x)$ gathers all the terms involving u as a factor and $\bar{y}_2(t,x)$ the remaining terms; thus, $\dot{p}(t)$ above can be written as (omitting arguments)

$$\dot{p}(t) = -\left(k + 2\frac{\bar{y}_1}{y}u + 2\frac{\bar{y}_2}{y}\right)p(t), \quad y \neq 0. \tag{5}$$

The Lyapunov function candidate $V(t,y) = 0.5y^2p(t)$ will be a legitimate Lyapunov function as long as $p(0) > 0$ and $p(t)$ is driven keeping its positivity. An easy way to do so consists in driving $p(t)$ to a positive constant value p_{ss}. Following standard methodology to this end [17][pg 197], the control structure is $u = u_s + u_{ss}$ where u_{ss} is the steady-state control that can maintain equilibrium at p_{ss} and $u_s = u - u_{ss}$ drives $p_s = p - p_{ss}$ to 0.

Solving u_{ss} from

$$0 = -\left(k + 2\frac{\bar{y}_1}{y}u_{ss} + 2\frac{\bar{y}_2}{y}\right)p_{ss},$$

yields

$$u_{ss} = -\left(\frac{ky}{2\bar{y}_1} + \frac{\bar{y}_2}{\bar{y}_1}\right). \tag{6}$$

As for u_s, it is calculated to stabilize the system

$$\dot{p}_s = -\left(k + 2\frac{\bar{y}_1}{y}(u_s + u_{ss}) + 2\frac{\bar{y}_2}{y}\right)(p_s + p_{ss}) = -2\frac{\bar{y}_1}{y}u_s(p_s + p_{ss}),$$

where the last expression is obtained taking into account u_{ss} in (6). A possible choice for u_s is thus $u_s = 100y(p_s - p_{ss})/\bar{y}_1$, as it ensures $p(t)$ is driven to p_{ss} as time goes to infinity. The final form of the duty cycle u is obtained adding up u_{ss} and u_s.

4.1.3. A dynamic quadratic Lyapunov function tracking a positive signal

Under the same considerations of the previous proposal, a Lyapunov function candidate $V(t, y) = 0.5y^2p(t)$ whose time derivative allows solving the dynamics of $p(t)$ as in (5), can be used. Exploiting the time-varying properties of $p(t)$ (namely, those of $V(t, y)$), which can be *any* continuous function as long as it is positive, is the purpose of the next development.

Consider the problem of tracking a desired positive function $p_d(t)$; the standard solution consists in defining the tracking error $e(t) = p(t) - p_d(t)$, whose time derivative $\dot{e}(t) = \dot{p}(t) - \dot{p}_d(t)$ is, upon substitution of $\dot{p}$ in (5),

$$\dot{e}(t) = -\left(k + 2\frac{\bar{y}_2}{y}\right)p(t) - 2\frac{\bar{y}_1}{y}p(t)u(t) - \dot{p}_d(t). \tag{7}$$

Thus, choosing the control input

$$u(t) = \frac{\left(k + 2\frac{\bar{y}_2}{y}\right)p(t) + \dot{p}_d(t) + v(t)}{-2\frac{\bar{y}_1}{y}p(t)} = \frac{(ky + 2\bar{y}_2)\,p(t) + y\dot{p}_d(t) + yv(t)}{-2\bar{y}_1 p(t)}, \tag{8}$$

with $v(t) = -k_e e(t)$, $k_e > 0$, reduces the error dynamics to $\dot{e}(t) = -k_e e(t)$, which means $e(t)$ asymptotically converges to zero as time goes to infinity.

4.2. Lyapunov-based numerical proposals

Two numerical proposals with different sets of nonlinearities are now developed; in contrast with those already presented, finding the control law as well as the Lyapunov function is no longer an analytical task, but a convex optimization problem in terms of LMIs. Although these conditions are only sufficient, systematicness is a clear advantage of the numerical approach.

4.2.1. A 1-nonlinearity LMI based solution

As in the last two proposals, a dynamic Lyapunov function candidate $V(t,y) = 0.5y^2p(t)$ whose time derivative allows solving the dynamics of $p(t)$ as in (5), is considered. Again, a positive function $p_d(t)$ is going to be tracked by the same techniques, i. e., defining the tracking error $e(t) = p(t) - p_d(t)$ and using its time derivative (7) as to solve u to leave a new system with input v. More specifically, adding and subtracting $(k + 2\bar{y}_2/y)p_d(t)$ to the error dynamics (7) yields

$$\begin{aligned}\dot{e}(t) &= -\left(k + 2\frac{\bar{y}_2}{y}\right)p(t) - 2\frac{\bar{y}_1}{y}p(t)u - \dot{p}_d(t) + \left(k + 2\frac{\bar{y}_2}{y}\right)p_d(t) - \left(k + 2\frac{\bar{y}_2}{y}\right)p_d(t)\\ &= -\left(k + \frac{2\bar{y}_2}{y}\right)e(t) - \frac{2\bar{y}_1}{y}p(t)u - \dot{p}_d(t) - \left(k + \frac{2\bar{y}_2}{y}\right)p_d(t).\end{aligned}$$

Applying the control input

$$u(t) = \frac{\dot{p}_d(t) + \left(k + 2\frac{\bar{y}_2}{y}\right)p_d(t) - v(t)}{-2\frac{\bar{y}_1}{y}p(t)} = \frac{y\dot{p}_d(t) + (ky + 2\bar{y}_2)\,p_d(t) - yv(t)}{-2\bar{y}_1 p(t)}, \tag{9}$$

with $v(t)$ as a new virtual input, reduces the error dynamics to the following nonlinear system:

$$\dot{e}(t) = -\left(k + 2\frac{\bar{y}_2}{y}\right)e(t) - v(t), \quad y \neq 0.$$

The nonlinear term $2\bar{y}_2/y$ depends on the state x_2, temperature $T(t)$, and irradiation $\lambda(t)$, thus, considering the bounds of the nonlinear term $z(t,x_2) = 2\bar{y}_2/y \in [z^0, z^1]$, it can be convexly rewritten by means of the nonlinear sector methodology [31] as follows

$$z(t,x_2) = \sum_{i=0}^{1} w_i(z)a_i, \;\; w_0(z) = \frac{z^1 - z}{z^1 - z^0}, \;\; w_1(z) = 1 - w_0(z),$$

with $a_i = (2\bar{y}_2/y)|_{w_i=1}$, $w_0(z) + w_1(z) = 1$, $0 \leq w_i \leq 1$, $i = \{0,1\}$. Then, considering the virtual control $v(t) = \sum_{i=0}^{1} w_i(z)k_{ei}e(t)$ the closed-loop of the error system can be written as

$$\dot{e}(t) = -\sum_{i=0}^{1} w_i(z)\,(k + a_i + k_{ei})\,e(t).$$

Therefore, the asymptotic stability of the origin is guaranteed if

$$-\sum_{i=0}^{1} w_i(z)\,(k + a_i + k_{ei}) < 0,$$

which in turn is guaranteed by the following LMIs

$$-(k + a_i + k_{ei}) < 0, \quad i = \{0,1\}. \tag{10}$$

4.2.2. A 2-nonlinearity LMI based solution

Consider again a Lyapunov function candidate $V(y) = 0.5y^2p(t)$, whose time derivative allows solving the dynamics of $p(t)$ as in (5). As in the two previous proposals, a positive function $p_d(t)$ is going to be tracked by the same techniques, i. e., defining the tracking error $e(t) = p(t) - p_d(t)$ whose time derivative is (7), then, considering $u(t) = 1 + \bar{u}(t)$ with $\bar{u}$ being a virtual input, the error dynamics (7) yield

$$\dot{e}(t) = -\left(k + 2\frac{\bar{y}_1}{y} + 2\frac{\bar{y}_2}{y}\right)p(t) - 2\frac{\bar{y}_1}{y}p(t)\bar{u} - \dot{p}_d(t),$$

adding and subtracting $(k + 2\bar{y}_1/y + 2\bar{y}_2/y)p_d(t)$ allows rearrange the error dynamic as

$$\dot{e}(t) = -\left(k + 2\frac{\bar{y}_1}{y} + 2\frac{\bar{y}_2}{y}\right)e(t) - \left(k + 2\frac{\bar{y}_1}{y} + 2\frac{\bar{y}_2}{y}\right)p_d(t) - 2\frac{\bar{y}_1}{y}p(t)\bar{u} - \dot{p}_d(t).$$

Thus, choosing the control input

$$\bar{u}(t) = \frac{-\dot{p}_d(t) - \left(k + 2\frac{\bar{y}_1}{y} + 2\frac{\bar{y}_2}{y}\right)p_d(t) + v(t)}{2\frac{\bar{y}_1}{y}p(t)} = \frac{-y\dot{p}_d(t) - (ky + 2\bar{y}_1 + 2\bar{y}_2)\,p_d(t) + yv(t)}{2\bar{y}_1 p(t)}, \tag{11}$$

with $v(t)$ as a new virtual input, the error dynamics are reduced to the following nonlinear system:

$$\dot{e}(t) = -\left(k + 2\frac{\bar{y}_1}{y} + 2\frac{\bar{y}_2}{y}\right)e(t) - v(t).$$

Nonlinear terms $2\bar{y}_1/y$ and $2\bar{y}_2/y$ depend on the states x_1, x_2 as well as on external signals $T(t)$ and $\lambda(t)$; thus, considering its bounds $z_1(t,x) = 2\bar{y}_1/y \in [z_1^0, z_1^1]$ and $z_2(t,x) = 2\bar{y}_2/y \in [z_2^0, z_2^1]$, they can be convexly rewritten by means of the nonlinear sector methodology as follows

$$z_1(t,x) = \sum_{i=0}^{1} w_i^1(z_1)a_i, \quad z_2(t,x) = \sum_{i=0}^{1} w_i^2(z_2)b_i,$$

$$w_0^1(z_1) = \frac{z_1^1 - z_1}{z_1^1 - z_1^0}, \quad w_1^1(z_1) = 1 - w_0^1(z_1), \quad w_0^2(z_2) = \frac{z_2^1 - z_2}{z_2^1 - z_2^0}, \quad w_1^2(z_2) = 1 - w_0^2(z_2),$$

with $a_i = (2\bar{y}_2/y)|_{w_i^1(z_1)=1}$, $b_i = (2\bar{y}_2/y)|_{w_i^2(z_2)=1}$, $w_0^j(z_j) + w_1^j(z_j) = 1$, $0 \le w_i^j \le 1$, $i = \{0,1\}$, $j = \{1,2\}$. In order to ease the notation let us define $\mathbb{B} = \{0,1\}$, $\mathbf{i} = (i_1, i_2) \in \mathbb{B}^2$, and $w_{\mathbf{i}}(z) = w_{i_1}^1 w_{i_2}^2$. Then, considering the virtual control $v(t) = \sum_{\mathbf{i}} w_{\mathbf{i}}(z)k_{e\mathbf{i}}e(t)$ the closed-loop of the error system can be written as

$$\dot{e}(t) = -\sum_{\mathbf{i}=(i_1,i_2)} w_{\mathbf{i}}(z)\,(k + a_{i_1} + b_{i_2} + k_{e\mathbf{i}})\,e(t).$$

Therefore, the asymptotic stability of the origin is guaranteed if

$$-\sum_{\mathbf{i}\in\mathbb{B}^2} w_{\mathbf{i}}(z)\,(k + a_{i_1} + b_{i_2} + k_{e\mathbf{i}}) < 0, \tag{12}$$

which in turn is guaranteed by the following LMIs

$$-(k+a_{i_1}+b_{i_2}+k_{e\mathbf{i}})<0,\ i_1,i_2=\{0,1\},\ \mathbf{i}\in\mathbb{B}^2. \tag{13}$$

Despite being scalar, the LMI-based methodologies just presented can straightforwardly incorporate decay rate, input/output constraints and $\mathscr{H}_\infty$ disturbance rejection by means of well known LMIs [7]; generalizations to non-scalar cases as those which use bidirectional converters can be easily adopted [20].

5. SIMULATION RESULTS

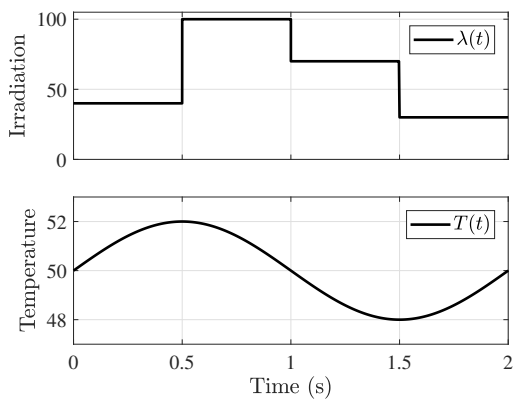

Fig. 3: Irradiation $\lambda(t)$ (mW/cm^2) and temperature $T(t)$ (°C) signals for simulation purposes.

The proposals developed in the previous section are put at test in the sequel; all of them solve the MPPT problem under time-varying temperature $T(t) = 50 + 2\sin(\pi t)$ and irradiation $\lambda(t) = 40(\mathscr{U}(t) - \mathscr{U}(t-0.5)) + 100(\mathscr{U}(t-0.5) - \mathscr{U}(t-1)) + 70(\mathscr{U}(t-1) - \mathscr{U}(t-1.5)) + 30(\mathscr{U}(t-1.5) - \mathscr{U}(t-2))$ (both shown in Figure 3) for the PV power system with buck converter in (1); parameters are taken as given in Table 2. All simulations consider initial conditions $x_1(0) = 1$A, $x_2(0) = 12$V, and $x_3(0) = 2$V.

Proposal 4.1.1 corresponds to a standard quadratic Lyapunov-based analytical solution, where the control input $u(t)$ is solved from (4) and applied to system (3) with gain $k = 50$. Time evolution of the states and PV power is shown in Figure 4a while the input and output signals are shown in Figure 4b; clearly, since output $y(t)$ is driven to 0 despite irradiation changes, the PV power achieves the maximum power point.

Proposal 4.1.2 uses a time-varying Lyapunov function $V(t,y) = 0.5y^2p(t)$ where $p(t)$ will be driven to $p_{ss} = 1$ from the initial condition $p(0) = 2$. The structure of the control input is $u(t) = u_s + u_{ss}$ with $u_s = 100y(p_s - p_{ss})/\bar{y}_1$ and u_{ss} as in (6), with $k = 50$. Figure 5a shows the time evolution of the states as well as the PV power; Figure 5b shows the control input $u(t)$ (duty cycle) and the output $y(t)$ (time derivative of the PV power with respect to voltage); finally Figure 5c shows how $p(t)$ goes to p_{ss} preserving the

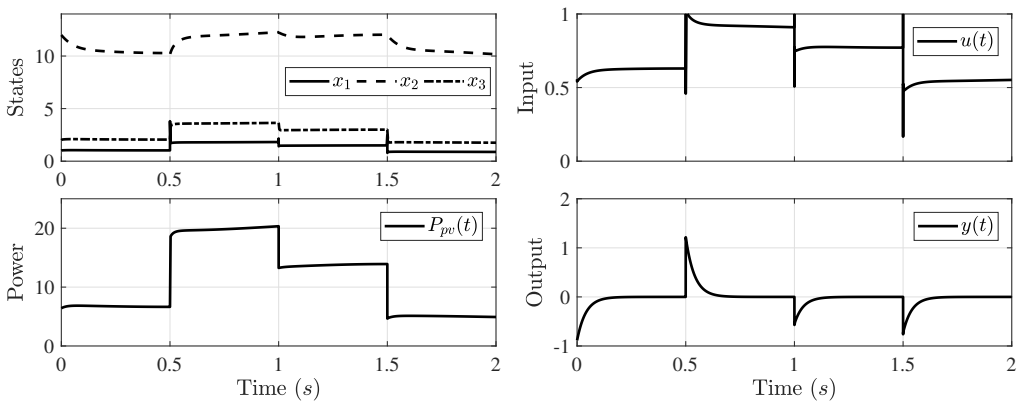

(a) Time evolution of states and PV power. (b) Control input and output signals.

Fig. 4: Simulation results of proposal 4.1.1.

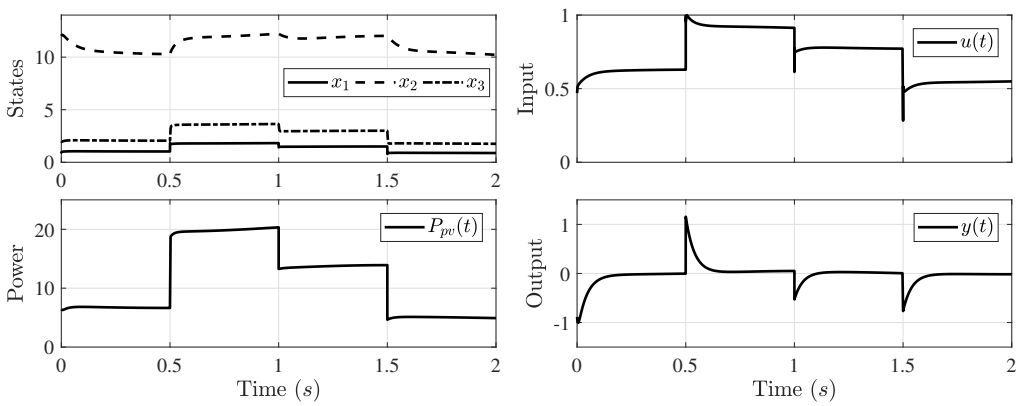

(a) Time evolution of states and PV power. (b) Control input and output signals.

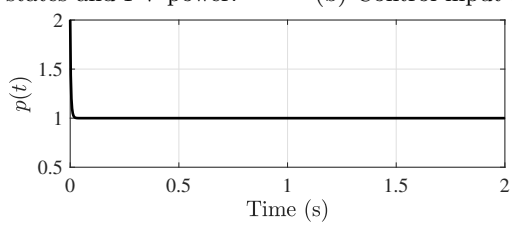

(c) Time evolution of signal $p(t)$.

Fig. 5: Simulation results of proposal 4.1.2.

Lyapunov function positive-definiteness. As expected, the MPPT problem is efficiently solved as proven by the way $y(t)$ is driven to 0 at every change of the external signals $\lambda(t)$ and $T(t)$.

Proposal 4.1.3 is very similar to the previous one in the sense that a dynamic Lyapunov function $V(t, y) = 0.5y^2p(t)$ is employed to infer a control law that drives the desired output $y(t)$ to 0, but instead of driving function $p(t)$ to a constant, it is shown that *any* positive function may work as well providing a richer family of solutions. To do so, gains $k = 50$ and $k_e = 20$ have been employed in control law (8) with a desired positive signal $p_d(t) = 0.1\sin(8t) + 1$ to be tracked by $p(t)$. Figure 6a shows the time evolution of the states as well as the PV power; Figure 6b shows the control $u(t)$ and the output $y(t)$; finally, Figure 6c shows $p(t)$ tracking the desired positive signal $p_d(t)$. Clearly, the maximum PV power is obtained when $y(t) = 0$.

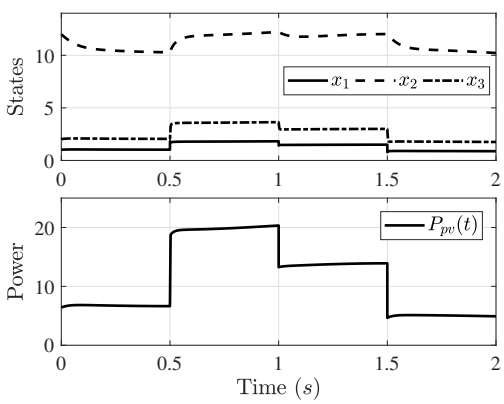

(a) Time evolution of states and PV power.

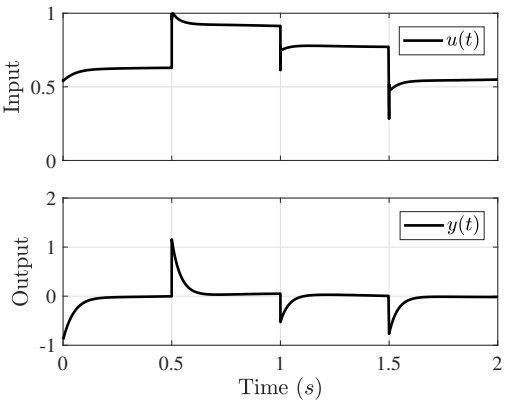

(b) Control input and output signals.

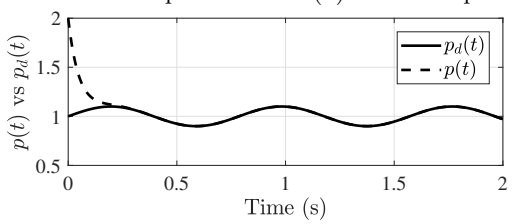

(c) Time evolution of signal $p(t)$ vs $p_d(t)$.

Fig. 6: Simulation results of proposal 4.1.3.

Proposal 4.2.1 corresponds to a numerical Lyapunov-based solution, i. e., the gains involved in the control law are calculated solving LMI conditions in the MATLAB$^{\text{TM}}$LMI-Toolbox [15]. Numerical advantages come at a price as a region of interest should be defined; in this case the region is defined by the state intervals $x_1 \in [-5, 5]$A and $x_2 \in [10, 20]$V for the inductance current and the PV voltage, respectively, as well as time-varying bounds $\lambda \in [30, 100]\text{mW/cm}^2$ and $T \in [48, 52]^\circ$C, for irradiation and temperature, respectively.

Based on these bounds, control law $v(t) = \sum_{i=0}^{1} w_i(z)k_{ei}e(t)$ is constructed: $w_i(z)$ are convex functions of the state; gains $k_{e0} = 132608$ and $k_{e1} = -43600$ are obtained from LMIs (10). Figure 7a shows the states and PV power; Figure 7b the control $u(t)$ and output $y(t)$; Figure 7c $p(t)$ tracking $p_d(t)$ for Lyapunov function $V(t, y) = 0.5y^2p(t)$. Clearly, the MPPT problem is solved as $y(t) = 0$ for every change in $\lambda(t)$ and $T(t)$.

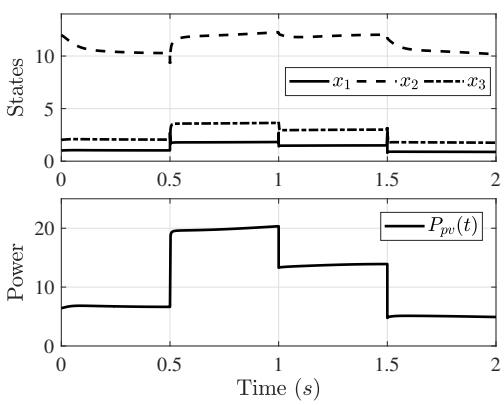

(a) Time evolution of states and PV power.

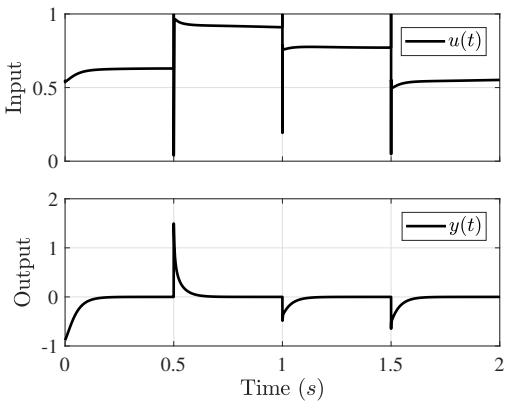

(b) Control input and output signals.

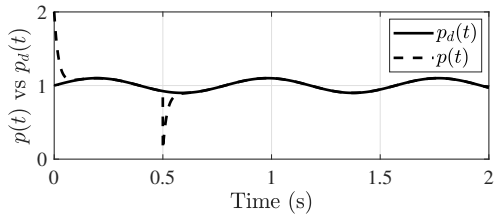

(c) Time evolution of signal $p(t)$ vs $p_d(t)$.

Fig. 7: Simulation results of proposal 4.2.1.

Proposal 4.2.2 considers a control law $u(t) = 1 + \bar{u}(t)$ with $\bar{u}$ as in (11) with $k = 100$ and a 2-nonlinearity PDC structure $v(t) = \sum_{i=0}^{1} w_i(z) k_{ei} e(t)$, whose gains $k_{e00} = 787026.86$, $k_{e01} = 490216.5$, $k_{e10} = -1639587.09$ and $k_{e11} = -1936397.45$ are calculated solving LMIs in (13). Figure 8a shows the states and PV power; Figure 8b the control $u(t)$ and output $y(t)$; Fig 8c tracking of $p_d(t)$ by $p(t)$. Again, these plots prove the MPPT problem is effectively solved.

Table 3 shows a detailed comparison among the five approaches developed in this work, showing the exact values of the control and output signals u and y, respectively, the input signal energy defined as $\int_0^t |u(t)|^2 dt$, and the photovoltaic power P_{pv} at five different time instants. Four of these time instants correspond to changes in the irradiation signal ($t = 0.0001$s, $t = 0.5001$s, $t = 1.001$s and $t = 1.5001$s) while that at $t = 0.9$s corresponds to a supposedly steady-state operation point. All approaches perform well in a similar manner, but some differences can be highlighted: numerical approaches provide greater power (perhaps due to the optimization in the LMI solver algorithm) and are the only ones that are able to bring output y to zero in steady state (see the rows corresponding to them at $t = 0.9$s).

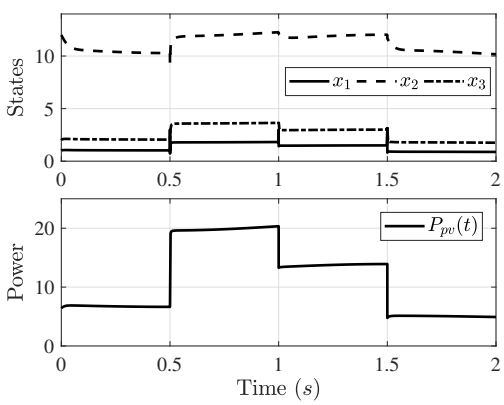

(a) Time evolution of states and PV power.

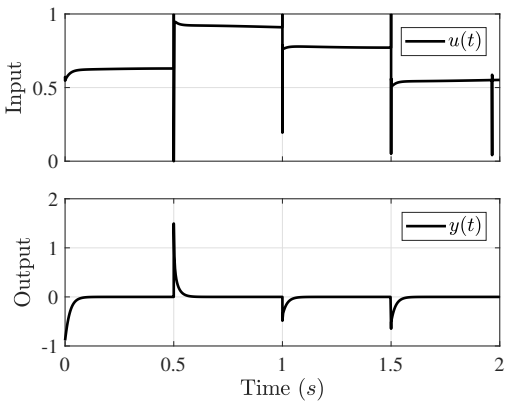

(b) Control input and output signals.

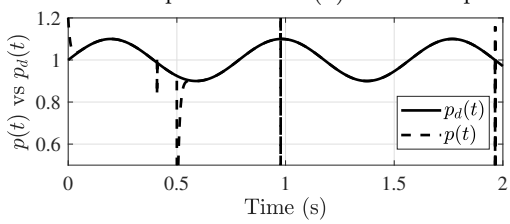

(c) Time evolution of signal $p(t)$ vs $p_d(t)$.

Fig. 8: Simulation results of proposal 4.2.2.

6. EXPERIMENTAL RESULTS

In order to validate the effectiveness of the Lyapunov-based approaches in real-time experiments, the work bench is shown in Figure 9. Two experiments corresponding to proposals 4.1.3 (analytical) and 4.2.2 (numerical) are now presented. In real-time implementations, controllers are implemented by a DSP-based control card, specifically the dSPACE DS1104. The frequency of the PWM signal is set to 100000Hz. The PV voltage, inductance current, and irradiation are sampled by the A/D converters and fed into the DSP card. To measure irradiation, the Kipp & Zonen SP Lite2 pyranometer was used, which has a sensitivity of $67.6\mu\text{V/W/m}^2$. Because the temperature during each experiment does not present significant changes, it was measured with a type K thermocouple at the beginning of each experiment and set as constant in the control laws.

Proposal 4.1.3: The implementation of the control law (8) with gains defined in the simulation section 5 yields the power response shown at the bottom of Figure 10a for the irradiance signal at the top of the same figure. As shown at the top of Figure 10b, the control signal is initially set at 0.95 in order to switch later to our control proposal and check the effect on the power and output responses, the latter seen going to 0 right after the control signal corresponding to our proposal is turned on (Figure 10b, bottom); therefore, since $y(t) \to 0$ the maximum power point is achieved.

time (s)	proposal	input u	output y	energy of u	power P_{pv}
0.0001	4.1.1	0.5413	-0.8831	29.599×10^{-6}	6.4159
	4.1.2	0.5066	-0.8919	24.951×10^{-6}	6.4076
	4.1.3	0.5392	-0.8836	29.318×10^{-6}	6.4154
	4.2.1	0.5384	-0.8742	29.009×10^{-6}	6.4234
	4.2.2	0.5509	-0.8486	30.394×10^{-6}	6.4470
0.5001	4.1.1	0.9456	1.2130	0.1921	18.4034
	4.1.2	0.9564	1.1528	0.1894	18.5684
	4.1.3	0.9566	1.1528	0.1902	18.5685
	4.2.1	0.9196	1.2782	0.1911	18.1984
	4.2.2	0.8697	1.1293	0.1943	18.6274
0.9	4.1.1	0.9136	0.0001	0.5364	20.1142
	4.1.2	0.9167	0.0464	0.5345	20.1133
	4.1.3	0.9167	0.0459	0.5354	20.1134
	4.2.1	0.9135	0	0.5319	20.1143
	4.2.2	0.9135	0	0.5330	20.1143
1.0001	4.1.1	0.7694	-0.5500	0.6195	13.2542
	4.1.2	0.7731	-0.5263	0.6182	13.2660
	4.1.3	0.7731	-0.5264	0.6191	13.2660
	4.2.1	0.7739	-0.3809	0.6150	13.3317
	4.2.2	0.7771	-0.3715	0.6161	13.3353
1.5001	4.1.1	0.5161	-0.7284	0.9175	4.6893
	4.1.2	0.5205	-0.7639	0.9179	4.6543
	4.1.3	0.5207	-0.7640	0.9188	4.6543
	4.2.1	0.5285	-0.5127	0.9137	4.8834
	4.2.2	0.5384	-0.5001	0.9158	4.8937

Tab. 3: Comparison between different approaches.

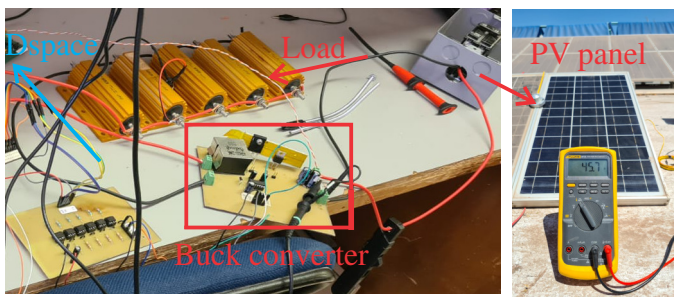

Fig. 9: Work bench for MPPT control.

Proposal 4.2.2: The implementation of the control law (11) with gains defined in the simulation section 5 are now presented. In contrast with the implementation shown before, this experiment was done under a higher irradiation signal as shown at the top

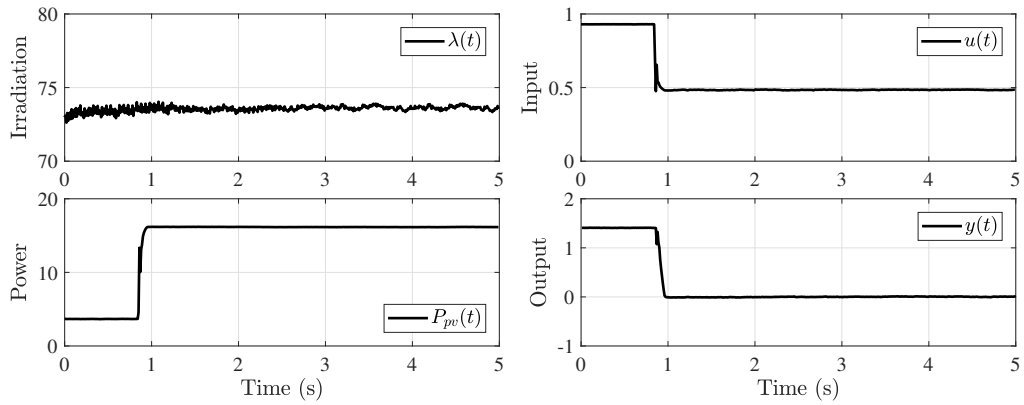

(a) Irradiation and PV power. (b) Control input and output signals.

Fig. 10: Implementation results of proposal 4.1.3.

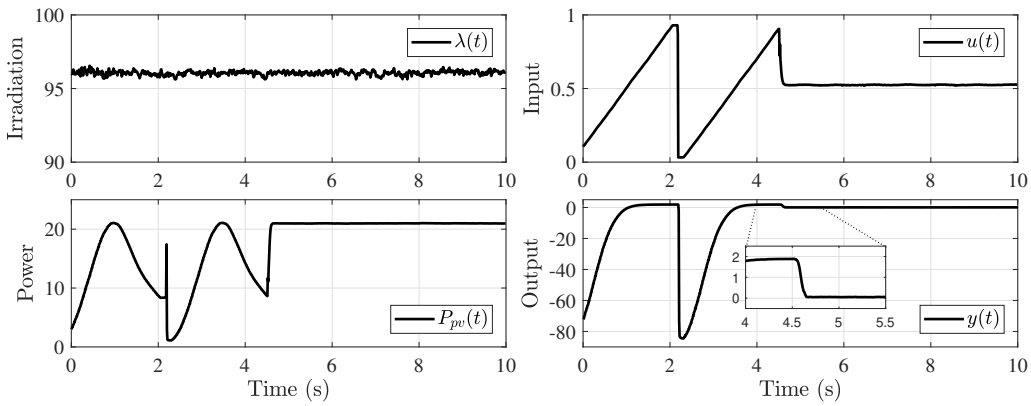

(a) Irradiation and PV power. (b) Control input and output signals.

Fig. 11: Implementation results of proposal 4.2.2.

of Figure 11a. Moreover, at the beginning of this experiment the control input is a ramp signal ranging from 0.05 to 0.95 as shown at the top of Figure 11b causing the power and output signals to oscillate as shown in the first four seconds at the bottom of Figs. 11a and 11b respectively. After this, our control proposal is introduced, driving the power to its maximum and keeping it there, as shown in Figure 11a (bottom). Also, it is easy to see at the bottom of Figure 11b that the output signal goes to zero when our control proposal takes over (a detailed subfigure is shown around this instant), which, as stated before, means that the maximum power point has been achieved.

Importantly, note that the proposals just presented are able to robustly deal with time-varying irradiation or temperature, without further adaptation in the control law structure.

7. CONCLUSIONS AND PERSPECTIVES

A novel family of Lyapunov-based controllers for solving the maximum power point tracking problem in a solar power generation system (composed by a stand-alone photovoltaic panel connected to a DC/DC buck converter) has been presented. Based on the fact that the maximum power point is achieved when its output, defined as the derivative of the photovoltaic power with respect to its voltage, is zero, analytically and numerically designed output-dependent Lyapunov functions, both state-dependent and time-varying, have been proven to be effective in designing the required duty cycle signal. Simulation and real-time results have been presented to put at test the proposals performance and implementability.

For future work, these results can be extended in the followings directions:

1. *DC/DC boost converters:* This class of systems can deal with other applications of importance, e. g., those requiring keeping high voltages instead of high currents. Lyapunov-based approaches may require higher dimension vectors than those above since the duty cycle u uses a different channel in the system.

2. *Time-varying parameters:* Aging, partial cloudiness, and other changes affecting parameters can be taken into account via nonlinear time-varying control, e. g., by means of $P(t)$ in the Lyapunov proposals.

3. *Fault-tolerant control:* Sensor and actuator failures –common in some of the aforementioned schemes can be dealt with using this sort of techniques.

4. *Observer-based control:* In order to reduce the number of sensors while keeping the formal Lyapunov analysis, a state observer could be used to reduce implementation costs.

5. *Robustness:* Control design able to deal with parametric uncertainties and/or disturbances in the same convex embedding/LMI framework.

ACKNOWLEDGEMENT

This work was supported by the CONACYT scholarship for CVU 731421, the ECOS Nord SEP CONACYT ANUIES Project 291309, and the ITSON PROFAPI Project 2023-CA-002.

(Received November 17, 2022)

REFERENCES

[1] A. Y. Abdelaziz and Y. Almoataz: Modern Maximum Power Point Tracking Techniques for Photovoltaic Energy Systems. Springer, 2020.

[2] M. M Algazar, H. A. El-Halim, M. E. El Kotb Salem, et al.: Maximum power point tracking using fuzzy logic control. Int. J. Electr.Power Energy Systems *39* (2012), 1, 21–28. DOI:10.1097/BPB.0b013e32834ee5f8

[3] Z. Artstein: Stabilization with relaxed controls. Nonlinear Analysis: Theory Methods Appl. *7* (1983), 11, 1163–1173. DOI:10.1016/0362-546X(83)90049-4

[4] A. B. G. Bahgat, N. H. Helwa, G. E. Ahmad, and E. T. El Shenawy: Maximum power point traking controller for pv systems using neural networks. Renewable Energy *30* (2008), 8, 1257–1268. DOI:10.3724/SP.J.1005.2008.01257

[5] J. Benedek, T.-T. Sebestyén, and B. Bartók: Evaluation of renewable energy sources in peripheral areas and renewable energy-based rural development. Renewable Sustainable Energy Rev. *90* (2018), 516–535. DOI:10.1016/j.rser.2018.03.020

[6] M. Bernal, P. Hušek, and V. Kučera: Non quadratic stabilization of continuous-time systems in the Takagi–Sugeno form. Kybernetika *42* (2006), 6, 665–672. DOI10.1007/s11003-006-0131-4

[7] M. Bernal, A. Sala, Z. Lendek, and T. M. Guerra: Analysis and Synthesis of Nonlinear Control Systems: A Convex Optimisation Approach. Springer, Cham 2022.

[8] K. R. Bharath and E. Suresh: Design and implementation of improved fractional open circuit voltage based maximum power point tracking algorithm for photovoltaic applications. Int. J. Renewable Energy Ress. (IJRER) *7* (2017), 3, 1108–1113.

[9] S. Boyd, L. El Ghaoui, E. Féron, and V. Balakrishnan: Linear Matrix Inequalities in System and Control Theory. Studies in Applied Mathematics *15*, Philadelphia 1994.

[10] Ch. S. Chiu: Ts fuzzy maximum power point tracking control of solar power generation systems. IEEE Trans. Energy Convers. *25* (2010). 4, 1123–1132. DOI:10.1109/TEC.2010.2041551

[11] Ch. S. Chiu and Y. L. Ouyang: Robust maximum power tracking control of uncertain photovoltaic systems: A unified ts fuzzy model-based approach. IEEE Trans. Control Systems Technol. *19* (2011), 6, 1516–1526. DOI:10.1109/tcst.2010.2093900

[12] Z. M, Dalala, Z. U. Zahid, W. Yu, Y. Cho, and J.-S. Lai: Design and analysis of an mppt technique for small-scale wind energy conversion systems. IEEE Trans. Energy Convers. *28* (2013), 3, 756–767. DOI:10.1109/TEC.2013.2259627

[13] M. A. Elgendy, B. Zahawi, and D. J. Atkinson: Assessment of the incremental conductance maximum power point tracking algorithm. IEEE Trans. Sustainable Energy *4* (2012), 1, :108–117. DOI:10.1109/TSTE.2012.2202698

[14] R. Faranda, S. Leva, and V. Maugeri: MPPT techniques for PV systems: Energetic and cost comparison. In: 2008 IEEE Power and Energy Society General Meeting-Conversion and Delivery of Electrical Energy in the 21st Century,IEEE 2008, pp. 1–6.

[15] P. Gahinet, A. Nemirovsky, A. J. Laub, and M. Chilali: LMI Control Toolbox. Math Works, Natick 1995.

[16] A. K. Gupta and R. Saxena: Review on widely-used MPPT techniques for PV applications. In: 2016 International Conference on Innovation and Challenges in Cyber Security (ICICCS-INBUSH), IEEE 2016, pp. 270–273. DOI:10.1109/ICICCS.2016.7542321

[17] H. K. Khalil: Nonlinear Control. Pearson Higher Ed, 2014.

[18] D. Lalili, A. Mellit, N. Lourci, B. Medjahed, and E. M. Berkouk: Input output feedback linearization control and variable step size mppt algorithm of a grid-connected photovoltaic inverter. Renewable Energy *36* (2011), 12, 3282–3291. DOI:10.1016/j.renene.2011.04.027

[19] Y. Mahmoud, M. Abdelwahed, and E. F. El-Saadany: An enhanced mppt method combining model-based and heuristic techniques. IEEE Trans. Sustainable Energy *7* (2015), 2, 76–585.

[20] M. Mao, L. Zhang, L. Yang, B. Chong, H. Huang, and L. Zhou: MPPT using modified salp swarm algorithm for multiple bidirectional pv-ćuk converter system under partial shading and module mismatching. Solar Energy *209* (2020), 334–349. DOI:10.1016/j.solener.2020.08.078

[21] Y. Mokhtari and D. Rekioua: High performance of maximum power point tracking using ant colony algorithm in wind turbine. Renewable Energy *126* (2018), 1055–1063. DOI:10.1016/j.renene.2018.03.049

[22] P. A. Owusu and S. Asumadu-Sarkodie: A review of renewable energy sources, sustainability issues and climate change mitigation. Cogent Engrg. *3* (2016), 1, 1167990. DOI:10.1080/23311916.2016.1167990

[23] A. Pandey, N. Dasgupta, and A. K. Mukerjee: High-performance algorithms for drift avoidance and fast tracking in solar mppt system. IEEE Trans. Energy Convers. *23* (2008), 2, 681–689. DOI:10.1109/TEC.2007.914201

[24] D. Pilakkat and S. Kanthalakshmi: An improved p&o algorithm integrated with artificial bee colony for photovoltaic systems under partial shading conditions. Solar Energy *178* (2019), 37–47. DOI:10.1016/j.solener.2018.12.008

[25] A. Qazi, F. Hussain, N. A. B. D. Rahim, G. Hardaker, D. Alghazzawi, K. Shaban, and K. Haruna: Towards sustainable energy: a systematic review of renewable energy sources, technologies, and public opinions. IEEE Acess *7* (2019), 63837–63851. DOI:10.1109/ACCESS.2019.2906402

[26] M. Salimi: Practical implementation of the lyapunov based nonlinear controller in dc-dc boost converter for mppt of the pv systems. Solar Energy *173* (2018), 246–255. DOI:10.1016/j.solener.2018.07.078

[27] A. Sandali, T. Oukhoya, and A. Cheriti: Modeling and design of pv grid connected system using a modified fractional short-circuit current mppt. In: 2014 International Renewable and Sustainable Energy Conference (IRSEC), IEEE 2014, pp. 224–229.

[28] D. Sera, L. Mathe, T. Kerekes, S. V. Spataru, and R. Teodorescu: On the perturb-and-observe and incremental conductance mppt methods for pv systems. IEEE J. Photovoltaics *3* (2013), 3, :1070–1078. DOI:10.1109/JPHOTOV.2013.2261118

[29] M. Sokolov and D. Shmilovitz: A modified mppt scheme for accelerated convergence. IEEE Trans. Energy Convers. *23* (2008), 4, 1105–1107. DOI:10.1109/TEC.2008.2001464

[30] E. D. Sontag: A universal construction of artstein's theorem on nonlinear stabilization. Systems Control Lett. *13* (1989), 2, 117–123. DOI:10.1016/0167-6911(89)90028-5

[31] T. Taniguchi, K. Tanaka, and H. O. Wang: Model contruction, rule reduction and robust compensation for generalized form of Takagi–Sugeno fuzzy systems. IEEE Trans. Fuzzy Systems *9* (2001), 4, 525–538. DOI:10.1109/91.940966

Jorge Álvarez, Sonora Institute of Technology, 5 de febrero 818 Sur, Ciudad Obregon, 85000. Mexico.

e-mail: jorge_kookee_04@hotmail.com

Jorge Ruiz, Sonora Institute of Technology, 5 de febrero 818 Sur, Ciudad Obregon, 85000. Mexico.

e-mail: jorgeruiz.c@gmail.com

Miguel Bernal, Sonora Institute of Technology, 5 de febrero 818 Sur, Ciudad Obregon, 85000. Mexico.

e-mail: miguel.bernal@itson.edu.mx